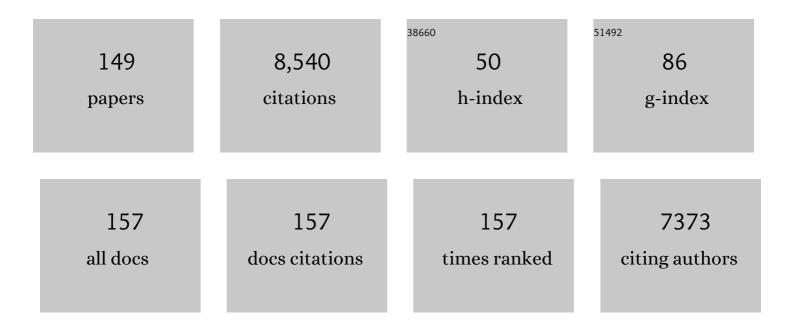
List of Publications by Year in descending order

Source: https://exaly.com/author-pdf/9439683/publications.pdf Version: 2024-02-01



#	Article	IF	CITATIONS
1	Understanding trends in electrochemical carbon dioxide reduction rates. Nature Communications, 2017, 8, 15438.	5.8	527
2	Conversion of amides to esters by the nickel-catalysed activation of amide C–N bonds. Nature, 2015, 524, 79-83.	13.7	479
3	Ligand-accelerated enantioselective methylene C(sp ³)–H bond activation. Science, 2016, 353, 1023-1027.	6.0	296
4	How Doped MoS ₂ Breaks Transition-Metal Scaling Relations for CO ₂ Electrochemical Reduction. ACS Catalysis, 2016, 6, 4428-4437.	5.5	254
5	Mechanisms and Origins of Switchable Chemoselectivity of Ni-Catalyzed C(aryl)–O and C(acyl)–O Activation of Aryl Esters with Phosphine Ligands. Journal of the American Chemical Society, 2014, 136, 2017-2025.	6.6	218
6	Palladium-Catalyzed Suzuki–Miyaura Coupling of Aryl Esters. Journal of the American Chemical Society, 2017, 139, 1311-1318.	6.6	212
7	Experimental–Computational Synergy for Selective Pd(II)-Catalyzed C–H Activation of Aryl and Alkyl Groups. Accounts of Chemical Research, 2017, 50, 2853-2860.	7.6	189
8	Enantioselective Synthesis of Atropisomers Featuring Pentatomic Heteroaromatics by Pd-Catalyzed C–H Alkynylation. ACS Catalysis, 2019, 9, 1956-1961.	5.5	174
9	Highly Chemoselective, Transition-Metal-Free Transamidation of Unactivated Amides and Direct Amidation of Alkyl Esters by N–C/O–C Cleavage. Journal of the American Chemical Society, 2019, 141, 11161-11172.	6.6	172
10	Isolated boron in zeolite for oxidative dehydrogenation of propane. Science, 2021, 372, 76-80.	6.0	155
11	Cu/Chiral Phosphoric Acid-Catalyzed Asymmetric Three-Component Radical-Initiated 1,2-Dicarbofunctionalization of Alkenes. Journal of the American Chemical Society, 2019, 141, 1074-1083.	6.6	151
12	Nickel-catalyzed amination of aryl carbamates and sequential site-selective cross-couplings. Chemical Science, 2011, 2, 1766.	3.7	148
13	Nickel atalyzed Activation of Acyl Câ^'O Bonds of Methyl Esters. Angewandte Chemie - International Edition, 2016, 55, 2810-2814.	7.2	142
14	Mechanisms and Origins of Chemo- and Regioselectivities of Ru(II)-Catalyzed Decarboxylative C–H Alkenylation of Aryl Carboxylic Acids with Alkynes: A Computational Study. Journal of the American Chemical Society, 2017, 139, 7224-7243.	6.6	134
15	Atroposelective Synthesis of Axially Chiral Styrenes via an Asymmetric C–H Functionalization Strategy. CheM, 2020, 6, 497-511.	5.8	133
16	Pillararene Host–Guest Complexation Induced Chirality Amplification: A New Way to Detect Cryptochiral Compounds. Angewandte Chemie - International Edition, 2020, 59, 10868-10872.	7.2	133
17	Iodoarene-Catalyzed Stereospecific Intramolecular sp ³ C–H Amination: Reaction Development and Mechanistic Insights. Journal of the American Chemical Society, 2015, 137, 7564-7567.	6.6	130
18	Copperâ€Catalyzed Enantioselective Markovnikov Protoboration of αâ€Olefins Enabled by a Buttressed Nâ€Heterocyclic Carbene Ligand. Angewandte Chemie - International Edition, 2018, 57, 1376-1380.	7.2	129

#	Article	IF	CITATIONS
19	Tuning the LUMO Energy of an Organic Interphase to Stabilize Lithium Metal Batteries. ACS Energy Letters, 2019, 4, 644-650.	8.8	129
20	Alternate Heme Ligation Steers Activity and Selectivity in Engineered Cytochrome P450-Catalyzed Carbene-Transfer Reactions. Journal of the American Chemical Society, 2018, 140, 16402-16407.	6.6	106
21	Mechanism and Origins of Ligand-Controlled Stereoselectivity of Ni-Catalyzed Suzuki–Miyaura Coupling with Benzylic Esters: AÂComputational Study. Journal of the American Chemical Society, 2017, 139, 12994-13005.	6.6	99
22	Cobalt-Catalyzed Asymmetric Synthesis of gem-Bis(silyl)alkanes by Double Hydrosilylation of Aliphatic Terminal Alkynes. CheM, 2019, 5, 881-895.	5.8	99
23	Palladium atalyzed Decarbonylative Borylation of Carboxylic Acids: Tuning Reaction Selectivity by Computation. Angewandte Chemie - International Edition, 2018, 57, 16721-16726.	7.2	98
24	Reactivity and Chemoselectivity of Allenes in Rh(I)-Catalyzed Intermolecular (5 + 2) Cycloadditions with Vinylcyclopropanes: Allene-Mediated Rhodacycle Formation Can Poison Rh(I)-Catalyzed Cycloadditions. Journal of the American Chemical Society, 2014, 136, 17273-17283.	6.6	96
25	The Origins of Dramatic Differences in Five-Membered vs Six-Membered Chelation of Pd(II) on Efficiency of C(sp ³)–H Bond Activation. Journal of the American Chemical Society, 2017, 139, 8514-8521.	6.6	96
26	Enantioselective Synthesis of Atropisomeric Anilides via Pd(II)-Catalyzed Asymmetric C–H Olefination. Journal of the American Chemical Society, 2020, 142, 18266-18276.	6.6	96
27	Distortion-accelerated cycloadditions and strain-release-promoted cycloreversions in the organocatalytic carbonyl-olefin metathesis. Chemical Science, 2014, 5, 471-475.	3.7	91
28	Nucleophile-Dependent <i>Z</i> / <i>E</i> - and Regioselectivity in the Palladium-Catalyzed Asymmetric Allylic C–H Alkylation of 1,4-Dienes. Journal of the American Chemical Society, 2019, 141, 5824-5834.	6.6	89
29	Trapping White Phosphorus within a Purely Organic Molecular Container Produced by Imine Condensation. Angewandte Chemie - International Edition, 2017, 56, 14545-14550.	7.2	85
30	Mechanism and Origins of Selectivity in Ru(II)-Catalyzed Intramolecular (5+2) Cycloadditions and Ene Reactions of Vinylcyclopropanes and Alkynes from Density Functional Theory. Journal of the American Chemical Society, 2013, 135, 6588-6600.	6.6	84
31	Factors Controlling the Reactivity and Chemoselectivity of Resonance Destabilized Amides in Ni-Catalyzed Decarbonylative and Nondecarbonylative Suzuki-Miyaura Coupling. Journal of the American Chemical Society, 2017, 139, 15522-15529.	6.6	84
32	Palladium-Catalyzed Selective Five-Fold Cascade Arylation of the 12-Vertex Monocarborane Anion by B–H Activation. Journal of the American Chemical Society, 2018, 140, 13798-13807.	6.6	79
33	Asymmetric dearomatization catalysed by chiral BrĄ̃nsted acids via activation of ynamides. Nature Chemistry, 2021, 13, 1093-1100.	6.6	77
34	Cp*Co(III)-Catalyzed Enantioselective Hydroarylation of Unactivated Terminal Alkenes via C–H Activation. Journal of the American Chemical Society, 2021, 143, 19112-19120.	6.6	73
35	Mechanism and Selectivity of <i>N</i> -Triflylphosphoramide Catalyzed (3 ⁺ + 2) Cycloaddition between Hydrazones and Alkenes. Journal of the American Chemical Society, 2014, 136, 13769-13780.	6.6	72
36	Organocatalytic Enantioselective Coniaâ€Eneâ€Type Carbocyclization of Ynamide Cyclohexanones: Regiodivergent Synthesis of Morphans and Normorphans. Angewandte Chemie - International Edition, 2019, 58, 16252-16259.	7.2	72

#	Article	IF	CITATIONS
37	Palladiumâ€Catalyzed Decarbonylative Borylation of Carboxylic Acids: Tuning Reaction Selectivity by Computation. Angewandte Chemie, 2018, 130, 16963-16968.	1.6	71
38	Synthesis of Biaryls via Decarbonylative Palladium-Catalyzed Suzuki-Miyaura Cross-Coupling of Carboxylic Acids. IScience, 2019, 19, 749-759.	1.9	71
39	Catalytic enantioselective desymmetrizing functionalization of alkyl radicals via Cu(i)/CPA cooperative catalysis. Nature Catalysis, 2020, 3, 401-410.	16.1	71
40	Mechanism and Origins of Ligand-Controlled Selectivities in [Ni(NHC)]-Catalyzed Intramolecular (5 +) Tj ETQq0 0 Society, 2013, 135, 1456-1462.	0 rgBT /O [.] 6.6	verlock 10 T 68
41	Role of Subsurface Oxygen on Cu Surfaces for CO ₂ Electrochemical Reduction. Journal of Physical Chemistry C, 2018, 122, 16209-16215.	1.5	68
42	Poly(thioether)s from Closed-System One-Pot Reaction of Carbonyl Sulfide and Epoxides by Organic Bases. Journal of the American Chemical Society, 2019, 141, 5490-5496.	6.6	68
43	Mechanism-based ligand design for copper-catalysed enantioconvergent C(sp3)–C(sp) cross-coupling of tertiary electrophiles with alkynes. Nature Chemistry, 2022, 14, 949-957.	6.6	68
44	Palladium-catalyzed decarbonylative Suzuki–Miyaura cross-coupling of amides by carbon–nitrogen bond activation. Chemical Science, 2019, 10, 9865-9871.	3.7	67
45	Predicting Regioselectivity in Radical Câ ^{~^} H Functionalization of Heterocycles through Machine Learning. Angewandte Chemie - International Edition, 2020, 59, 13253-13259.	7.2	65
46	Bimetallic Cooperative Catalysis for Decarbonylative Heteroarylation of Carboxylic Acids via Câ€O/Câ€H Coupling. Angewandte Chemie - International Edition, 2021, 60, 10690-10699.	7.2	64
47	Synthesis of Axially Chiral <i>N</i> â€Arylindoles via Atroposelective Cyclization of Ynamides Catalyzed by Chiral BrÃ,nsted Acids. Angewandte Chemie - International Edition, 2022, 61, .	7.2	60
48	An axial-to-axial chirality transfer strategy for atroposelective construction of C–N axial chirality. CheM, 2021, 7, 1917-1932.	5.8	59
49	Distortion-Controlled Reactivity and Molecular Dynamics of Dehydro-Diels–Alder Reactions. Journal of the American Chemical Society, 2016, 138, 8247-8252.	6.6	57
50	Iron-Catalyzed Hydroboration of Vinylcyclopropanes. Organic Letters, 2017, 19, 5422-5425.	2.4	56
51	Total Syntheses of Rhodomolleins XX and XXII: A Reductive Epoxideâ€Opening/Beckwith–Dowd Approach. Angewandte Chemie - International Edition, 2019, 58, 8556-8560.	7.2	56
52	Stereoretentive C(<i>sp</i> ³)–S Cross-Coupling. Journal of the American Chemical Society, 2018, 140, 18140-18150.	6.6	55
53	Rhodium(III)-Catalyzed Asymmetric Borylative Cyclization of Cyclohexadienone-Containing 1,6-Dienes: An Experimental and DFT Study. Journal of the American Chemical Society, 2019, 141, 12770-12779.	6.6	52
54	Why Alkynyl Substituents Dramatically Accelerate Hexadehydro-Diels–Alder (HDDA) Reactions: Stepwise Mechanisms of HDDA Cycloadditions. Organic Letters, 2014, 16, 5702-5705.	2.4	51

#	Article	IF	CITATIONS
55	Computational Exploration of Mechanism and Selectivities of (NHC)Nickel(II)hydride-Catalyzed Hydroalkenylations of Styrene with α-Olefins. ACS Catalysis, 2015, 5, 5545-5555.	5.5	50
56	Divergent rhodium-catalyzed electrochemical vinylic C–H annulation of acrylamides with alkynes. Nature Communications, 2021, 12, 930.	5.8	48
57	Nickel-Catalyzed Alkyl–Alkyl Cross-Electrophile Coupling Reaction of 1,3-Dimesylates for the Synthesis of Alkylcyclopropanes. Journal of the American Chemical Society, 2020, 142, 5017-5023.	6.6	47
58	Selective Separation of Phenanthrene from Aromatic Isomer Mixtures by a Water-Soluble Azobenzene-Based Macrocycle. Journal of the American Chemical Society, 2021, 143, 3081-3085.	6.6	47
59	Highly-chemoselective step-down reduction of carboxylic acids to aromatic hydrocarbons <i>via</i> palladium catalysis. Chemical Science, 2019, 10, 5736-5742.	3.7	45
60	Dearomative 1,4-difunctionalization of naphthalenes via palladium-catalyzed tandem Heck/Suzuki coupling reaction. Nature Communications, 2020, 11, 4380.	5.8	45
61	Atroposelective synthesis of <i>N</i> -aryl peptoid atropisomers <i>via</i> a palladium(<scp>ii</scp>)-catalyzed asymmetric C–H alkynylation strategy. Chemical Science, 2021, 12, 9391-9397.	3.7	45
62	Nickel-Catalyzed Kumada Coupling of Boc-Activated Aromatic Amines via Nondirected Selective Aryl C–N Bond Cleavage. Organic Letters, 2019, 21, 1226-1231.	2.4	44
63	Versatility of Boron-Mediated Coupling Reaction of Oxetanes and Epoxides with CO ₂ : Selective Synthesis of Cyclic Carbonates or Linear Polycarbonates. ACS Sustainable Chemistry and Engineering, 2020, 8, 13056-13063.	3.2	44
64	Catalytic asymmetric synthesis of chiral trisubstituted heteroaromatic allenes from 1,3-enynes. Communications Chemistry, 2018, 1, .	2.0	43
65	Azobenzeneâ€Based Macrocyclic Arenes: Synthesis, Crystal Structures, and Light ontrolled Molecular Encapsulation and Release. Angewandte Chemie - International Edition, 2021, 60, 5766-5770.	7.2	43
66	Decarbonylative Phosphorylation of Carboxylic Acids via Redox-Neutral Palladium Catalysis. Organic Letters, 2019, 21, 9256-9261.	2.4	42
67	A Unified Explanation for Chemoselectivity and Stereospecificity of Ni-Catalyzed Kumada and Cross-Electrophile Coupling Reactions of Benzylic Ethers: A Combined Computational and Experimental Study. Journal of the American Chemical Society, 2019, 141, 5835-5855.	6.6	41
68	Catalytic and Photochemical Strategies to Stabilized Radicals Based on Anomeric Nucleophiles. Journal of the American Chemical Society, 2020, 142, 11102-11113.	6.6	39
69	Computational studies on Ni-catalyzed amide C–N bond activation. Chemical Communications, 2019, 55, 11330-11341.	2.2	37
70	Diastereoselective olefin amidoacylation <i>via</i> photoredox PCET/nickel-dual catalysis: reaction scope and mechanistic insights. Chemical Science, 2020, 11, 4131-4137.	3.7	37
71	Nickel atalyzed Activation of Acyl Câ^'O Bonds of Methyl Esters. Angewandte Chemie, 2016, 128, 2860-2864.	1.6	36
72	Ni-mediated C–N activation of amides and derived catalytic transformations. Science China Chemistry, 2017, 60, 1413-1424.	4.2	36

#	Article	IF	CITATIONS
73	Copperâ€Catalyzed Enantioselective Markovnikov Protoboration of αâ€Olefins Enabled by a Buttressed Nâ€Heterocyclic Carbene Ligand. Angewandte Chemie, 2018, 130, 1390-1394.	1.6	36
74	Constraining Homo- and Heteroanion Dimers in Ultraclose Proximity within a Self-Assembled Hexacationic Cage. Journal of the American Chemical Society, 2020, 142, 20182-20190.	6.6	36
75	Temperature-dependent self-assembly of a purely organic cage in water. Chemical Communications, 2018, 54, 3138-3141.	2.2	34
76	Mechanism and Selectivity Control in Ni- and Pd-Catalyzed Cross-Couplings Involving Carbon–Oxygen Bond Activation. Accounts of Chemical Research, 2021, 54, 2158-2171.	7.6	33
77	Reactivity Profiles of Diazo Amides, Esters, and Ketones in Transition-Metal-Free C–H Insertion Reactions. Journal of the American Chemical Society, 2019, 141, 3558-3565.	6.6	31
78	Ni(NHC)]-Catalyzed Cycloaddition of Diynes and Tropone: Apparent Enone Cycloaddition Involving an 8i€ Insertion. Journal of the American Chemical Society, 2014, 136, 17844-17851.	6.6	30
79	Coulombic-enhanced hetero radical pairing interactions. Nature Communications, 2018, 9, 1961.	5.8	30
80	Direct Synthesis of Aluminosilicate IWR Zeolite from a Strong Interaction between Zeolite Framework and Organic Template. Journal of the American Chemical Society, 2019, 141, 18318-18324.	6.6	30
81	Lowâ€Temperature Nickelâ€Catalyzed Câ^'N Crossâ€Coupling via Kinetic Resolution Enabled by a Bulky and Flexible Chiral <i>N</i> â€Heterocyclic Carbene Ligand. Angewandte Chemie - International Edition, 2021, 60, 16077-16084.	7.2	30
82	Mechanistic Insights into Two-Phase Radical C–H Arylations. ACS Central Science, 2015, 1, 456-462.	5.3	29
83	Trapping White Phosphorus within a Purely Organic Molecular Container Produced by Imine Condensation. Angewandte Chemie, 2017, 129, 14737-14742.	1.6	29
84	Mechanism and Origins of Chemo- and Regioselectivities of Pd-Catalyzed Intermolecular σ-Bond Exchange between Benzocyclobutenones and Silacyclobutanes: A Computational Study. Organometallics, 2018, 37, 592-602.	1.1	29
85	Decarbonylative Suzuki–Miyaura Cross-Coupling of Aroyl Chlorides. Organic Letters, 2020, 22, 6434-6440.	2.4	27
86	Kinetic Resolution of Tertiary Benzyl Alcohols via Palladium/Chiral Norbornene Cooperative Catalysis. Angewandte Chemie - International Edition, 2021, 60, 12824-12828.	7.2	27
87	Mechanism and Dynamics of Intramolecular C–H Insertion Reactions of 1-Aza-2-azoniaallene Salts. Journal of the American Chemical Society, 2015, 137, 9100-9107.	6.6	25
88	Rhodium-Catalyzed Asymmetric Addition of Organoboronic Acids to Aldimines Using Chiral Spiro Monophosphite-Olefin Ligands: Method Development and Mechanistic Studies. Journal of Organic Chemistry, 2018, 83, 11873-11885.	1.7	25
89	Design of Hemilabile N,N,N-Ligands in Copper-Catalyzed Enantioconvergent Radical Cross-Coupling of Benzyl/Propargyl Halides with Alkenylboronate Esters. Journal of the American Chemical Society, 2022, 144, 6442-6452.	6.6	25
90	How Tethers Control the Chemo- and Regioselectivities of Intramolecular Cycloadditions between Aryl-1-aza-2-azoniaallenes and Alkenes. Organic Letters, 2014, 16, 4260-4263.	2.4	24

#	Article	IF	CITATIONS
91	C–H Acidity and Arene Nucleophilicity as Orthogonal Control of Chemoselectivity in Dual C–H Bond Activation. Organic Letters, 2019, 21, 2360-2364.	2.4	24
92	Optically Active Flavaglines-Inspired Molecules by a Palladium-Catalyzed Decarboxylative Dearomative Asymmetric Allylic Alkylation. Journal of the American Chemical Society, 2020, 142, 12039-12045.	6.6	23
93	Computational studies on Ni-catalyzed Câ^'O bond activation of esters. Journal of Organometallic Chemistry, 2018, 864, 68-80.	0.8	22
94	Total Syntheses of (+)â€Sarcophytin, (+)â€Chatancin, (â^')â€3â€Oxochatancin, and (â^')â€Pavidolideâ€B: A Dive Approach. Angewandte Chemie - International Edition, 2019, 58, 5100-5104.	ergent 7:2	22
95	Engineered Cytochrome c-Catalyzed Lactone-Carbene B–H Insertion. Synlett, 2019, 30, 378-382.	1.0	22
96	Iron-Catalyzed Asymmetric Hydrosilylation of Vinylcyclopropanes via Stereospecific C-C Bond Cleavage. IScience, 2020, 23, 100985.	1.9	22
97	Direct Synthesis of Ketones from Methyl Esters by Nickelâ€Catalyzed Suzuki–Miyaura Coupling. Angewandte Chemie - International Edition, 2021, 60, 13476-13483.	7.2	22
98	Ir(III)-Catalyzed Asymmetric C–H Activation/Annulation of Sulfoximines Assisted by the Hydrogen-Bonding Interaction. ACS Catalysis, 2022, 12, 9083-9091.	5.5	22
99	Generalized ionothermal synthesis of silica-based zeolites. Microporous and Mesoporous Materials, 2019, 286, 163-168.	2.2	21
100	Towards Dataâ€Ðriven Design of Asymmetric Hydrogenation of Olefins: Database and Hierarchical Learning. Angewandte Chemie - International Edition, 2021, 60, 22804-22811.	7.2	21
101	N-heterocyclic Carbene–Cu-Catalyzed Enantioselective Conjugate Additions with Alkenylboronic Esters as Nucleophiles. ACS Catalysis, 2017, 7, 5693-5698.	5.5	20
102	Carboxylate breaks the arene C–H bond <i>via</i> a hydrogen-atom-transfer mechanism in electrochemical cobalt catalysis. Chemical Science, 2020, 11, 5790-5796.	3.7	19
103	Chemoselective Transamidation of Thioamides by Transitionâ€Metalâ€Free Nâ^'C(S) Transacylation. Angewandte Chemie - International Edition, 2022, 61, .	7.2	19
104	Computational Study of Mechanism and Thermodynamics of Ni/IPr-Catalyzed Amidation of Esters. Molecules, 2018, 23, 2681.	1.7	18
105	Aluminum-Catalyzed Selective Hydroboration of Alkenes and Alkynylsilanes. Organic Process Research and Development, 2019, 23, 1703-1708.	1.3	18
106	How Solvents Control the Stereospecificity of Ni-Catalyzed Miyaura Borylation of Allylic Pivalates. ACS Catalysis, 2019, 9, 9589-9598.	5.5	18
107	Cobalt atalyzed Asymmetric Sequential Hydroboration/Isomerization/Hydroboration of 2â€Aryl Vinylcyclopropanes. Angewandte Chemie - International Edition, 2022, 61, .	7.2	18
108	A double-site Lewis pair for highly active and living synthesis of sulfur-containing polymers. Polymer Chemistry, 2019, 10, 6555-6560.	1.9	17

#	Article	IF	CITATIONS
109	Ligand-Controlled Diastereoselective 1,3-Dipolar Cycloadditions of Azomethine Ylides with Methacrylonitrile. Organic Letters, 2015, 17, 6166-6169.	2.4	16
110	The mechanism and regioselectivities of (NHC)nickel(ii)hydride-catalyzed cycloisomerization of dienes: a computational study. Organic and Biomolecular Chemistry, 2017, 15, 7131-7139.	1.5	16
111	Mechanism, Reactivity, and Selectivity of Nickel-Catalyzed [4 + 4 + 2] Cycloadditions of Dienes and Alkynes. Journal of Organic Chemistry, 2014, 79, 12177-12184.	1.7	15
112	Engaging Sulfonamides: Intramolecular Cross-Electrophile Coupling Reaction of Sulfonamides with Alkyl Chlorides. Journal of Organic Chemistry, 2020, 85, 1775-1793.	1.7	15
113	N-Heterocyclic Carbene–Cu-Catalyzed Enantioselective Allenyl Conjugate Addition. Organic Letters, 2018, 20, 6896-6900.	2.4	14
114	Migratory Aptitudes in Rearrangements of Destabilized Vinyl Cations. Journal of Organic Chemistry, 2019, 84, 15154-15164.	1.7	14
115	Predicting Regioselectivity in Radical Câ^'H Functionalization of Heterocycles through Machine Learning. Angewandte Chemie, 2020, 132, 13355-13361.	1.6	14
116	Copper atalyzed Enantioselective Hydroboration of 1,1â€Disubstituted Alkenes: Method Development, Applications and Mechanistic Studies. Asian Journal of Organic Chemistry, 2018, 7, 103-106.	1.3	13
117	Enantioselective Intramolecular Desymmetric αâ€Addition of Cyclohexanone to Propiolamide Catalyzed by Sodium L â€Prolinate. Chinese Journal of Chemistry, 2019, 37, 63-70.	2.6	13
118	Rhodium(III)-Catalyzed Asymmetric Reductive Cyclization of Cyclohexadienone-Containing 1,6-Dienes via an Anti-Michael/Michael Cascade Process. ACS Catalysis, 2021, 11, 8015-8022.	5.5	13
119	An Exception to the Carothers Equation Caused by the Accelerated Chain Extension in a Pd/Ag Cocatalyzed Cross Dehydrogenative Coupling Polymerization. Journal of the American Chemical Society, 2022, 144, 2311-2322.	6.6	13
120	A 3D Analogue of Phenyllithium: Solutionâ€Phase, Solidâ€State, and Computational Study of the Lithiacarborane [Liâ^'CB ₁₁ H ₁₁] ^{â^'} . Angewandte Chemie - International Edition, 2019, 58, 19007-19013.	7.2	12
121	Machine learning prediction of hydrogen atom transfer reactivity in photoredox-mediated C–H functionalization. Organic Chemistry Frontiers, 2021, 8, 6187-6195.	2.3	12
122	Synthesis of Axially Chiral <i>N</i> â€Arylindoles via Atroposelective Cyclization of Ynamides Catalyzed by Chiral BrÃ,nsted Acids. Angewandte Chemie, 0, , .	1.6	11
123	Directed B–H functionalization of the <i>closo</i> -dodecaborate cluster <i>via</i> concerted iodination–deprotonation: reaction mechanism and origins of regioselectivity. Organic Chemistry Frontiers, 2020, 7, 3648-3655.	2.3	10
124	Entropic Path Sampling: Computational Protocol to Evaluate Entropic Profile along a Reaction Path. Journal of Physical Chemistry Letters, 2021, 12, 10713-10719.	2.1	10
125	Computational studies of cinchona alkaloid-catalyzed asymmetric Michael additions. Chinese Chemical Letters, 2018, 29, 1585-1590.	4.8	9
126	A diquat-containing macrocyclic anion acceptor in pure water. Chemical Communications, 2019, 55, 8297-8300.	2.2	9

#	Article	IF	CITATIONS
127	Formation of phytosterol photooxidation products: A chemical reaction mechanism for light-induced oxidation. Food Chemistry, 2020, 333, 127430.	4.2	9
128	Understanding the mechanism and reactivity of Pd-catalyzed C–P bond metathesis of aryl phosphines: a computational study. Organic and Biomolecular Chemistry, 2020, 18, 5414-5419.	1.5	8
129	Understanding the Structureâ€Activity Relationship of Niâ€Catalyzed Amide Câ^'N Bond Activation using Distortion/Interaction Analysis. ChemCatChem, 2021, 13, 3536-3542.	1.8	8
130	Stepwise versus Concerted Reductive Elimination Mechanisms in the Carbon–Iodide Bond Formation of (DPEphos)RhMeI ₂ Complex. Organometallics, 2018, 37, 4711-4719.	1.1	7
131	Understanding the axial chirality control of quinidine-derived ammonium cation-directed O-alkylation: a computational study. Organic and Biomolecular Chemistry, 2019, 17, 1916-1923.	1.5	7
132	A [1 ₅]paracyclophenone and its fluorenone-containing derivatives: syntheses and binding to nerve agent mimics <i>via</i> aryl-CH hydrogen bonding interactions. Organic Chemistry Frontiers, 2021, 8, 25-31.	2.3	7
133	Bimetallic Cooperative Catalysis for Decarbonylative Heteroarylation of Carboxylic Acids via Câ€O/Câ€H Coupling. Angewandte Chemie, 2021, 133, 10785-10794.	1.6	7
134	Direct Synthesis of Ketones from Methyl Esters by Nickelâ€Catalyzed Suzuki–Miyaura Coupling. Angewandte Chemie, 2021, 133, 13588-13595.	1.6	7
135	Unexpected Stability of CO-Coordinated Palladacycle in Bidentate Auxiliary Directed C(sp ³)–H Bond Activation: A Combined Experimental and Computational Study. Organometallics, 2019, 38, 2022-2030.	1.1	6
136	Machine Learning Prediction of <scp>Structureâ€Performance</scp> Relationship in Organic Synthesis. Chinese Journal of Chemistry, 2022, 40, 2106-2117.	2.6	6
137	Synthesis of Aluminophosphate Molecular Sieves in Alkaline Media. Chemistry - A European Journal, 2020, 26, 11408-11411.	1.7	5
138	Scaling relationships and volcano plots of homogeneous transition metal catalysis. Dalton Transactions, 2020, 49, 3652-3657.	1.6	5
139	A Molecular Stereostructure Descriptor Based On Spherical Projection. Synlett, 2021, 32, 1837-1842.	1.0	5
140	Nickel-Catalyzed Domino Cross-Electrophile Coupling Dicarbofunctionalization Reaction To Afford Vinylcyclopropanes. ACS Catalysis, 2021, 11, 14369-14380.	5.5	5
141	Cobalt-Catalyzed Migration Isomerization of Dienes. Organic Letters, 2022, 24, 4592-4597.	2.4	5
142	Computation-Guided Development of the "Click―ortho-Quinone Methide Cycloaddition with Improved Kinetics. Organic Letters, 2020, 22, 2920-2924.	2.4	4
143	(2+1)-Cycloaddition Reactions Give Further Evidence of the Nitrenium-like Character of 1-Aza-2-azoniaallene Salts. Journal of Organic Chemistry, 2017, 82, 4001-4005.	1.7	3
144	The Distortion/Interaction Model for Analysis of Activation Energies of Organic Reactions. , 2018, , 371-402.		3

Χιν Ηονς

#	Article	IF	CITATIONS
145	Lowâ€Temperature Nickelâ€Catalyzed Câ^'N Crossâ€Coupling via Kinetic Resolution Enabled by a Bulky and Flexible Chiral N â€Heterocyclic Carbene Ligand. Angewandte Chemie, 2021, 133, 16213-16220.	1.6	3
146	Towards Dataâ€Driven Design of Asymmetric Hydrogenation of Olefins: Database and Hierarchical Learning. Angewandte Chemie, 2021, 133, 22986-22993.	1.6	3
147	Chemoselective Transamidation of Thioamides by Transitionâ€Metalâ€Free N–C(S) Transacylation. Angewandte Chemie, 0, , .	1.6	2
148	Divergent pathway and reactivity control of intramolecular arene C–H vinylation by vinyl cations. Organic and Biomolecular Chemistry, 2019, 17, 9135-9139.	1.5	1
149	Cobaltâ€Catalyzed Asymmetric Sequential Hydroboration/Isomerization/Hydroboration of 2â€Aryl Vinylcyclopropanes. Angewandte Chemie, 0, , .	1.6	0